The Astrophysical Journal, 700:1042–1046, 2009 August 1 doi:10.1088/0004-637X/700/2/1042

ENERGY-DEPENDENT TIME LAGS IN THE SEYFERT 1 GALAXY NGC 4593

K. Sriram[1], V. K. Agrawal[2,3], and A. R. Rao[3]
[1] Department of Astronomy, Osmania University, Hyderabad 500 07, India; astrosriram@yahoo.co.in
[2] Indian Space Research Organization, HQ., BEL Road, Bangalore 560 094, India
[3] Tata Institute of Fundamental Research, Mumbai 400005, India
Received 2009 January 31; accepted 2009 May 22; published 2009 July 8

ABSTRACT

We investigate the energy–time lag dependence of the source NGC 4593 using *XMM-Newton*/EPIC pn data. We found that the time lag dependency is linear in nature with respect to the logarithm of different energy bands. We also investigate the frequency-dependent time lags and identify that at some frequency range (5×10^{-5} Hz to 2×10^{-4} Hz) the X-ray emission is highly coherent, mildly frequency dependent, and very strongly energy dependent. These observations can be explained in the framework of the thermal Comptonization process, and they indicate a truncated accretion disk very close to the black hole. We discuss the plausible spectral state to explain the phenomenon and conclude that the observed properties bear a close resemblance to the intermediate state or the steep power-law state, found in galactic black hole sources.

Key words: accretion, accretion disks – black hole physics – galaxies: individual (NGC 4593) – galaxies: Seyfert

1. INTRODUCTION

It has become increasingly clear in recent times that the central engines of active galactic nuclei (AGNs) are magnified forms of galactic black hole candidates (GBHCs; McHardy et al. 2006). The scaled up X-ray timing and spectral variability characteristics in AGNs (with respect to GBHCs) indicate a common energy generation process in these sources. State transition in GBHCs is a common phenomenon whereas in AGNs, if scaled with mass, the state transition may occur in thousand to millions of years depending on the mass of the black hole. A detailed temporal and spectral study of a sample of AGNs, however, may shed light on the spectral states in AGNs. The cross spectrum as well as the power spectral density (PSD) of Ark 564 (Arevalo et al. 2006; McHardy et al. 2007) indicates that the source is in a very high state, and a double break in PSD and large separation between breaks also argue against a low/hard state like that seen in Cyg X-1 (Papadakis et al. 2002; Done & Gierlinski 2005). The very high accretion rate inferred in Ark564 (Romano et al. 2004) strongly suggests a very high state in this source. Detailed temporal studies indicate that the Seyfert galaxies NGC 3227, NGC 4051, and MGC-6-30-15 are in the high-soft state (McHardy et al. 2004, 2005; Uttley & McHardy 2005). The temporal properties of NGC 3783 and NGC 4258 suggest that these sources are in the low-hard state (Markowitz et al. 2003; Markowitz & Uttley 2005). An investigation of the PSD of NGC 3783 in a wider frequency range, however, showed that the PSD is consistent with a soft state model (Summons et al. 2007). Recent investigations have revealed that type 1 radio-quiet AGN and radio-loud AGN spectral states are analogous to the very high spectral state of GBHCs (Sobolewska et al. 2009).

One of the very interesting and important spectral states in GBHCs is the very high state, which is often observed during the transition from the low-hard state to the high-soft state (McClintock & Remillard 2004; Remillard & McClintock 2006; Done et al. 2007). This state is characterized by the presence of a steep power-law (SPL) component (with power-law index $\Gamma > 2.5$), which dominates the total observed X-ray flux, and hence this state is also referred to as the SPL state. This state was first seen in GX 339-4 and later observed in many other GBHCs (Miyamoto et al. 1993; Done et al. 2007). Quasi-periodic oscillations in the frequency range 0.1–30 Hz are also a common property of this state (McClintock & Remillard 2004). The study of hardness–intensity diagram of various black hole sources suggests the onset of relativistic jet during this transition state (Belloni et al. 2005). A theoretical modeling of X-ray spectra in the very high state of the XTE J1550-564 suggests that the disk is truncated and the inner part of accretion disk is filled with hot and compact central corona (Done & Kubota 2006). Anticorrelated hard lags were also discovered in XTE J1550-564, which favors a hot compact central corona in the very high state of this source (Sriram et al. 2007).

It is very important to identify such states in AGNs. Phenomenologically, one of the defining characteristics of such states is the existence of a confined compact corona, which is the source of the hard X-ray power law due to inverse Compton scattering of soft photons (Sunyaev & Titarchuk 1980). One of the ways to understand such a process is to study the time lags between two different energy bands. If the basic process is Comptonization, the soft photons gain energy because of fewer number of scattering with hot electrons present in the corona, and as the energy difference increases between two energy bands, the time lag also increases. This energy gain timescale have been measured in a few AGNs, NGC 7469 (Papadakis et al. 2001), MCG6-30-15 (Vaughan et al. 2003), NGC 4051 (McHardy et al. 2004), NGC 3783 (Markowitz 2005), and Mrk 110 (Dasgupta & Rao 2006). Similar type of energy-dependent lag was observed in GBHC, Cyg X-1 (Cui et al. 1997; Crary et al. 1998; Nowak et al. 1999b). This clearly indicates an underlying common radiative phenomenon in both GBHCs and AGNs. But this scenario of uniform Comptonization is, however, challenged by the study of Fourier-dependent lags. The Fourier study suggests that the low and high frequency variation may be because of different X-ray emitting regions in the accretion disk and also can be explained by a Compton cloud of radial dependence of electron density (Kazanas et al. 1997). Brenneman et al. (2007) have found a hard delay of the order of ∼230 s by cross correlating soft and hard X-ray bands in NGC 4593. Here, we try to investigate this observation further by making a detailed energy-dependent and frequency-dependent analysis of the delay.

NGC 4593 is a barred spiral galaxy of Hubble type SBb, which hosts Seyfert 1 nucleus situated toward the constellation Virgo. It is a close by galaxy at a redshift of $z = 0.009$

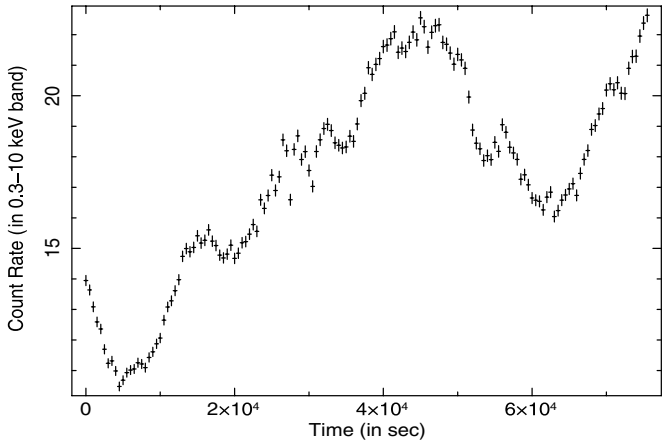

Figure 1. *XMM-Newton* PN 0.3–10 keV light curve of NGC 4593 binned at 50 s.

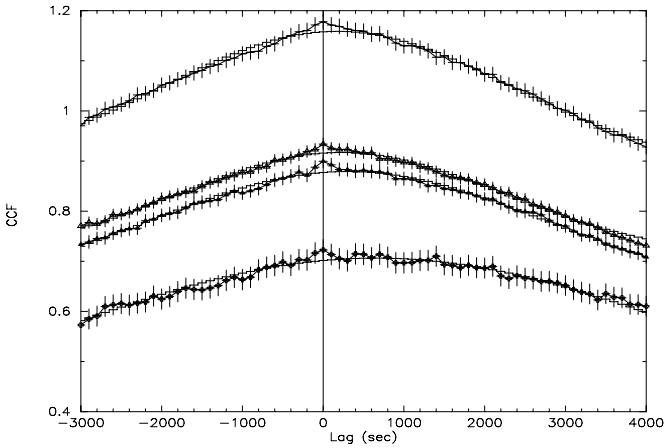

Figure 2. CCF in various energy bands with respect to the soft band (0.30–0.50 keV) is shown for NGC 4593. The energy bands are 0.50–0.80 keV, 0.80–1.50 keV, 1.50–4.0 keV, and 4.0–10.0 keV, respectively, from the top. The first (top) CCF is vertically shifted up by 0.3 for clarity. The continuous lines are Gaussian fits, and the vertical line at zero highlights the observed delay.

and an apparent visual magnitude of 11.67, and harbors a supermassive black hole of mass of the order of $8.1 \times 10^6\ M_\odot$ (Gebhardt et al. 2000)—which is consistent with the poorly constrained reverberation mapping estimate of $< 1.4 \times 10^7\ M_\odot$ (Peterson et al. 2004). NGC 4593 is highly variable in X-ray, UV, optical, and IR bands (Santos-Lleo et al. 1995) implying toward a variable continuum source close to the black hole. Multiband spectral energy distribution of NGC 4593 suggests that the respective accretion disk is truncated and the innermost region is dominated by ADAF (Lu & Wang 2000). The X-ray continuum is well fitted with photoabsorbed power law above 2 keV and shows spectral complexity behavior below this energy. The standard relativistic iron line is absent as well as reflection component is not seen, instead it has two narrow Fe Kα lines at 6.4 keV and 6.97 keV in the X-ray continuum (Brenneman et al. 2007; Reynolds et al. 2004). Because of missing relativistic spectral features in X-ray band, the geometry of NGC 4593 is speculated to be different from traditional geometry of AGNs or relativistic features may be buried in the noise as discussed by Reynolds et al. (2004).

In this paper, we make a detailed investigations of temporal properties of narrow line Seyfert 1 galaxy NGC 4593 using $\sim$ 70 ks data obtained by *XMM-Newton* observatory.

2. DATA REDUCTION AND ANALYSIS

NGC 4593 was observed on 2002 June 23 by *XMM-Newton* satellite. We have used EPIC pn camera data during which it was operating in a small window mode with medium filter. We have taken observation data files (ODF) to obtain the light curves of the source. Source photons were extracted from 40 $\times$ 40 arcsec^2 region and equal area is taken for collecting background photons, away from the source. The *epatplot* task gave no indication of pile-up during the observation. We have selected single and double events for the analysis (PATTERN $\lesssim$ 4 and FLAG = 0). The light curves are binned for 50 s and the XRONOS package is used for studying the temporal behavior of the source.

2.1. Energy-Dependent Lag

We have extracted the light curves in five different energy bands (0.3–0.5 keV, 0.5–0.8 keV, 0.8–1.5 keV, 1.5–4.0 keV, and 4.0–10 keV). During the observation, the source was highly variable and showed two dips separated by a steep increase. Initially, the average count rate was $\sim$ 12 s^{-1} followed by a steep increase to $\sim$ 25 s^{-1}. This is followed by a dip of around $\sim$ 18 s^{-1} and settled down at $\sim$ 25 s^{-1} (see Figure 1). To know the time lag in various energy bands, we have used the *crosscor* program to evaluate the cross correlation function (CCF) and the respective delay in the various energy bands. We have cross correlated the hard X-ray bands with the soft X-ray band (0.3–0.5 keV), and the results are shown in Figure 2. A Gaussian model was used to evaluate the time lags, and errors are estimated using the criteria $\Delta\chi^2 = 4$ (see Dasgupta & Rao 2006 and Table 1). The mean energy, given in Table 1, is the weighted mean for all the photons in each energy band. It was found that the magnitude of the lag is increasing as the energy bands are becoming harder with respect to 0.3–0.5 keV band. It clearly suggests that the photons take relatively more time to become relatively harder, most probably due to more number of scatterings (Figure 3).

Table 1
Details of the Selected Energy Bands and Time Lags

Correlated Energy Bands (keV)	Mean Energy (keV)	Time Lag (s)
0.30–0.50 vs. 0.50–0.80	0.64	171.00 ± 54.0
0.30–0.50 vs. 0.80–1.50	1.11	223.43 ± 55.0
0.30–0.50 vs. 1.50–4.0	2.29	305.00 ± 58.5
0.30–0.50 vs. 4.0–10.0	5.87	652.91 ± 91.0

2.2. Frequency-Dependent Lag

If $X_1(f)$ and $X_2(f)$ are Fourier transforms of two light curves in energy bands E_1 and E_2, then cross spectrum is defined as $C(f) = X_1^*(f)X_2(f)$. Time lag at frequency f is given by $\delta t = \arg[C(f)]/2\pi f$. If $S_1(f)$ and $S_2(f)$ are source powers in two different energy bands and $N_1(f)$ and $N_1(f)$ are noise spectra in same bands, then coherence function can be defined as

$$\gamma^2(f) = \frac{|\langle C(f)\rangle|^2 - N^2}{\langle |S_1(f)|^2\rangle \langle |S_2(f)|^2\rangle}, \quad (1)$$

where

$$N^2 = [|S_1(f)|^2|N_2(f)|^2 + |S_2(f)|^2|N_1(f)|^2 + |N_1(f)|^2|N_2(f)|^2]/m, \quad (2)$$

where m is the number of independent measurements (Vaughan & Nowak 1997). The error in coherence is calculated by the

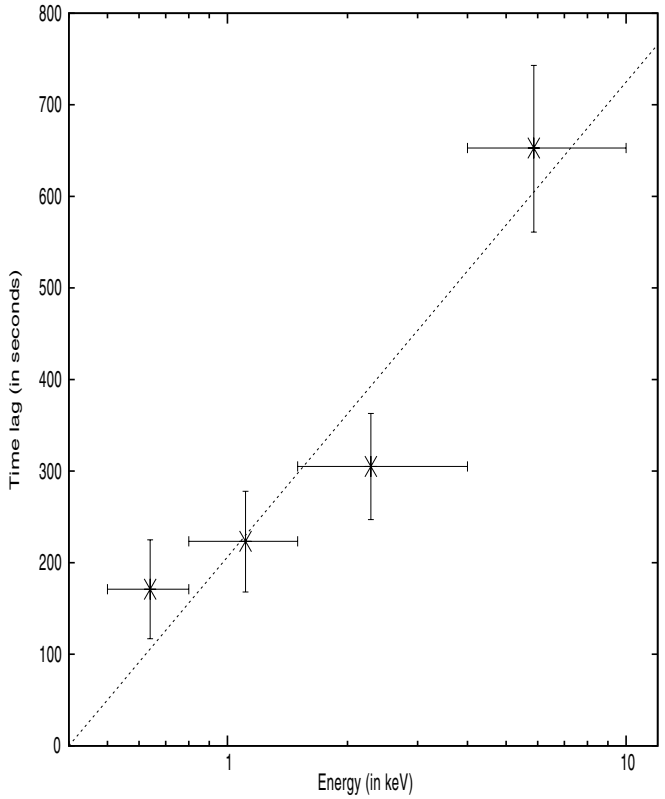

Figure 3. Observed time lags are plotted vs. energy for NGC 4593. The straight line corresponds to the thermal Comptonization model fit (see the text).

method described in (Nowak et al. 1999a, 1999b), and the error in the lags are calculated using the method described in Bendat & Piersol (1986). To estimate error bars on coherence, we used high power and high measured coherence limit. We re-binned the cross spectral density logarithmically and then computed the coherence and lag. In Figure 4, we show the coherence between 0.3–0.5 keV and 0.8–1.5 keV band light curves as a function of frequency. It is clear from this figure that the coherence drops above 5×10^{-4} Hz. The power spectrum also becomes noisy above this frequency (see Figure 5). Hence, we investigate the nature of lag spectrum in the frequency range 5×10^{-5}–5×10^{-4} Hz. We also compute cross-spectra between two different energy bands 0.3–0.5 keV versus 0.8–1.5 keV and 0.3–0.5 keV versus 4.0–10.0 keV. Frequency-dependent lag is shown in Figure 6 and it is evident in the figure that the lag scales up with energy separation.

3. DISCUSSION AND CONCLUSION

3.1. Energy-Dependent Lag From Comptonization

In this paper, we investigated the dependence of time lag on energy of the observed X-ray radiation in NGC 4593. Our results suggest that the time lag increases with the mean energy of observed photons. A similar dependence of lag on energy has been seen in other AGNs as well, and the observed lag is interpreted as Compton scattering time-scale (Dasgupta & Rao 2006). If this lag is due to the process of Comptonization, we can get some useful constraints on the geometry of the inner accretion disk. We note here that the Comptonization model applies to the energy-dependent lags measured at high temporal frequencies.

Let R be the size of the region in which the Comptonization process is undergoing. If λ is the mean free path of the photon

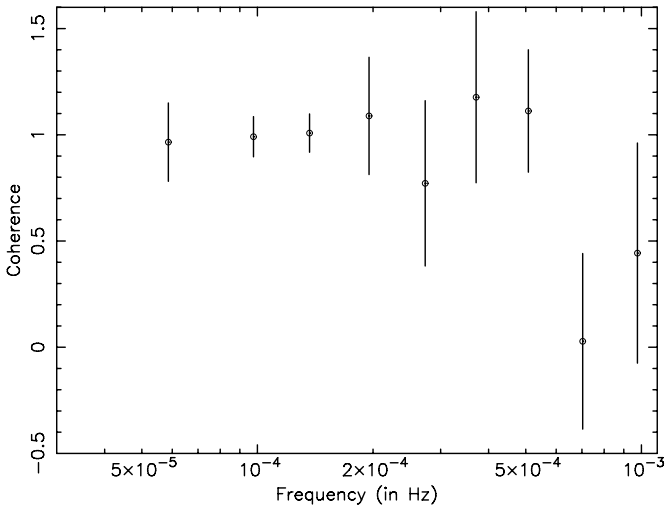

Figure 4. Coherence function calculated using energy bands 0.3–0.5 keV and 0.8–1.5 keV.

and τ_T is the optical depth of the plasma in this region, then the Comptonization time-scale will be given by

$$t_{\rm Comp} = \frac{\lambda}{c \times \max(1, \tau_T)}. \quad (3)$$

Let us assume E_0 to be the initial energy of the photon and after N scattering it attains an energy E_N (where $N = 1, 2, 3, 4$), i.e., $E_N = E_0 \times A^N$, where $A = 1 + 4\Theta + 16\Theta^2$ (known as the amplification factor and $\Theta = kT_e/m_ec^2$). Then the Comptonization time-scale can also be written in terms of the time lag and N as

$$t_{\rm Comp} = \frac{\tau_{\rm lag}}{N}, \quad (4)$$

where $\tau_{\rm lag}$ is the respective time lag.

The size of the region, in which the Comptonization process is undergoing, is equivalent to the distance traveled by the photons (i.e., λ, valid only if the medium is optically thin, i.e., $\max(1, \tau_T) \sim 1$). Using the above two equations, we get a Comptonizing region size of the order of $\sim 6 \times 10^{12}$ cm (using $\tau_{\rm lag} = 600$ s, for the 0.3–0.5 keV and 4–10 keV bands).

The observed time lags are nothing but the product of Comptonization time-scale and difference of successive number of scattering, which can be given by

$$\tau_{\rm lag} = \frac{R}{c \times \max(1, \tau_T)} \frac{\ln\left(\frac{E_N}{E_1}\right)}{\ln A}. \quad (5)$$

The observed time lag increases linearly with logarithm of energy (see Figure 3). Hence, the above equation suggests that the Comptonization process is responsible for the observed lag. We have fitted the above equation to the observed energy-dependent time lag (see Figure 3) and found that the size of the hard X-ray emitting region is $\sim 10^{13}$ cm and when the mass is taken as $7 \times 10^6\ M_\odot$ black hole (Nelson et al. 2004), R comes out to be $\sim 5R_g$.

3.2. Disk Geometry and Time Lag Spectrum

The geometry of the accretion disk in NGC 4593 is quite peculiar on the basis of Fe line (Brenneman et al. 2007; Reynolds et al. 2004). Also iron line does not show significant variation on the observed time span and are very narrow which are suggestive

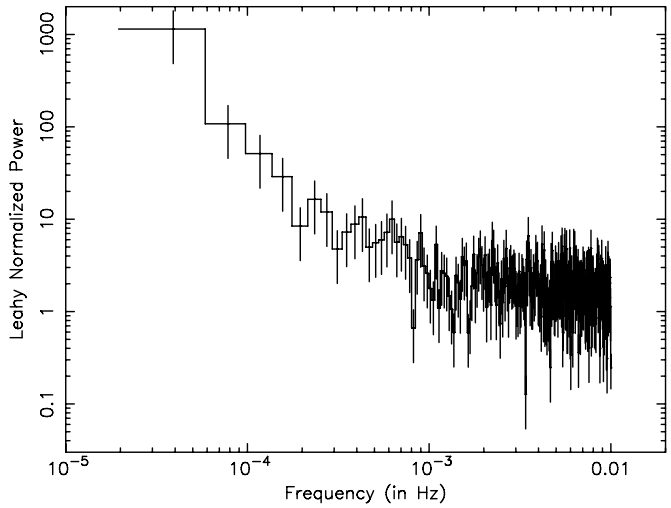

Figure 5. Power density spectrum (PDS) of NGC 4593 in the 0.8–1.5 keV energy band.

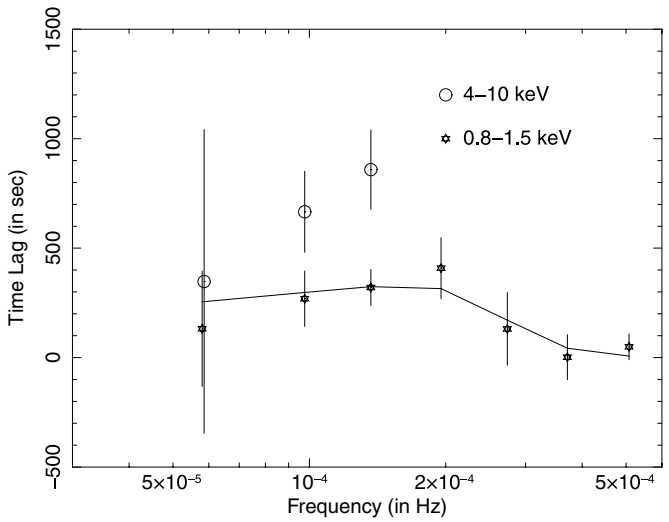

Figure 6. Frequency-dependent lag between 0.3–0.5 keV vs. 0.8–1.5 keV and 0.3–0.5 keV vs. 4.0–10.0 keV energy bands. The line shows the broken power-law fit (see the text).

of the absence of optically thick cold matter in the central 1000 R_g region. The inner 1000 R_g region may contain radiatively inefficient and hot optically thin plasma. The observed time lag suggests that there is also a compact central corona with a size of $\sim 5R_g$. The derived Compton cloud size from time lag suggests that most of the hard X-ray photons are emitted within $\sim 3R_g$ region. It has also been argued that NGC 4593 has a truncated accretion disk with a two-component flow of a geometrically thin disk and an advection-dominated flow within the truncation radius, a model commonly invoked to explain the low-hard and intermediate states of GBHs (Lu & Wang 2000). The intermediate state is characterized by a SPL component and a truncated accretion disk (with the truncation radius less than that found in the low-hard state). Though the power-law index is not steeper than that found in other Seyfert galaxies (Brenneman et al. 2007), the available data strongly suggest a thin disk converting into an advection-dominated central part, a configuration similar to the low-hard and intermediate states of GBHs.

Cross spectral analysis reveals that the lag observed in this source depends upon the Fourier frequency. The lag spectrum computed using the energy bands 0.3–0.5 keV and 0.8–1.5 keV reveals a broad peak in the frequency range 5×10^{-5}–5×10^{-4} Hz (see Figure 6). In this frequency range, the X-ray emission at different energies is highly coherent (see Figure 4). The lag spectrum, however, shows quite strong energy dependency. The structure in the lag spectrum can be fitted with a broken power law with first slope $\alpha = 0.3$ and second slope $\beta = -5$ with a $\chi^2 = 1.5$ for 3 degree of freedom (dof), an improvement in χ^2 of ~ 10 from a fit to a constant value. The break is observed at the frequency $f_b = 2.2 \times 10^{-4}$ Hz. The observed lag at different frequencies increases with the energy separation. The lag spectrum of Ark 564 shows step-like features (McHardy et al. 2007), and at higher frequencies, it can also be fitted with a broken power law (Arevalo et al. 2006). In Ark 564 also, the lag at different frequencies scales up with the energy separation. The lags below the break frequency are constant in NGC 4593, which is quite different from the trend of lag decreasing with increasing Fourier frequency seen in other sources such as MCG-6-30-25 (Vaughan et al. 2003), Mkn766 (Markowitz et al. 2007), and NGC 4051 (McHardy et al. 2004). The fractional lag in this frequency range is 1%–6%, which is similar to the fractional lag seen in the very high state of Cyg X-1.

If the energy-dependent lag is mainly due to Comptonization, then the bulk of the variability (confined to below 2×10^{-4} Hz, see Figure 6) is nearly frequency independent. It is quite possible that there is another variability component operating particularly above the break frequency $f_b = 2.2 \times 10^{-4}$ Hz, possibly from accretion disk fluctuations propagating from outside (see below). The spectral analysis of NGC 4593 suggests that the soft excess too can be modeled as due to Comptonization from a cooler plasma (Brenneman et al. 2007). It is quite possible that there is a hot compact central corona within a few Swartzchild radius (responsible for the bulk of the radiation and giving rise to the frequency-independent delays), surrounded by an optically thin plasma cloud extending to several hundred Swartzchild radius (responsible for the soft excess). There is a possibility that electron density in optically thin corona is varying with radius. It was suggested that if corona has nonuniform electron density, then the observed frequency dependence lag can be explained (Kazanas et al. 1997). There is also a possibility that there exist several different patches of hot Compton cloud (Sobolewska et al. 2004) giving rise to different time lags at different time-scales.

Another promising model, which explains the observed lag spectrum in Mrk 335 (Arevalo et al. 2008), is the fluctuations propagation model (Lyubarskii 1997; Kotov et al. 2001), which can also give energy-dependent delays. This model assumes that fluctuations in the accretion flow are produced at different radial distances from putative black hole. These fluctuations propagate on viscous time-scales and also assume that spectra harden toward the center. Kotov et al. (2001) have computed phase lags for different scenarios, which can explain the time lags caused by accretion. The lag spectrum observed in NGC 4593 is similar to that obtained for the freely falling blob model (see Figure 9 of Kotov et al. 2001), but the strong energy dependency, however, favors a Comptonization model.

We thank the anonymous referee for the very useful comments. This work has made use of observations obtained with *XMM-Newton*, an ESA science mission with instrumentation and contributions directly funded by ESA member states and the USA (NASA). The authors are grateful to Surajit Dasgupta for useful suggestions. K.S. is supported by the UGC through

the RFSMS scheme and thankful to TIFR for providing the facility to carry out the work.

REFERENCES

Arevalo, P., McHardy, I. M., & Summons, D. P. 2008, MNRAS, 388, 211
Arevalo, P., Papadakis, I. E., Uttley, P., McHardy, I. M., & Brinkmann, W. 2006, MNRAS, 372, 401
Belloni, et al. 2005, A&A, 440, 207
Bendat, J., & Piersol, A. 1986, Random Data: Analysis and Measurement Procedures (New York: Wiley)
Brenneman, L. W., et al. 2007, ApJ, 666, 817
Crary, D. J., et al. 1998, ApJ, 493, 71
Cui, W., Zhang, S. N., Focke, W., & Swank, J. H. 1997, ApJ, 484, 383
Dasgupta, S., & Rao, A. R. 2006, ApJ, 651, L13
Done, C., & Gierlinski, M. 2005, MNRAS, 364, 208
Done, C., Gierlinski, M., & Kubota, A. 2007, A&AR, 15, 1
Done, C., & Kubota, A. 2006, MNRAS, 371, 1216
Gebhardt, K., et al. 2000, ApJ, 543, L5
Kazanas, D., Hua, X., & Titarchuk, L. 1997, ApJ, 480, 735
Kotov, O., Churazov, E., & Gilfanov, M. 2001, MNRAS, 327, 799
Lu, Y., & Wang, T. 2000, ApJ, 537, L103
Lyubarskii, Y. E. 1997, MNRAS, 292, 679
Markowitz, A. 2005, ApJ, 635, 180
Markowitz, A., Papadakis, I., Arévalo, P., Turner, T. J., Miller, L., & Reeves, J. N. 2007, ApJ, 656, 116
Markowitz, A., & Uttley, P. 2005, ApJ, 625, 39
Markowitz, A., et al. 2003, ApJ, 593, 96
McClintock, J. E., & Remillard, R. A. 2004, in Compact Stellar X-Ray Sources, ed. W. H. G. Lewin & M. van der Klis (Cambridge: Cambridge Univ. Press), 157
McHardy, I. M., Gunn, K., Uttely, P., & Goad, M. R. 2005, MNRAS, 359, 1469
McHardy, I. M., Koerding, E., Knigge, C., Uttely, P., & Fender, R. P. 2006, Nature, 444, 730
McHardy, I. M., Papadakis, I. E., Uttely, P., Page, M., & Mason, K. O. 2004, MNRAS, 348, 783
McHardy, I. M., et al. 2007, MNRAS, 382, 985
Miyamoto, S., Iga, S., Kitamoto, S., & Karnado, Y. 1993, ApJ, 403, L39
Nelson, C. H., Green, R. F., Bower, G., Gebhardt, K., & Weistrop, D. 2004, ApJ, 615, 652
Nowak, M. A., Vaughan, B. A., Wilms, J., Dove, J. B., & Begelman, M. C. 1999a, ApJ, 510, 874
Nowak, M. A., Wilms, J., Vaughan, B. A., Dove, J. B., & Begelman, M. C. 1999b, ApJ, 515, 726
Papadakis, I. E., Brinkmann, W., Negoro, H., & Gliozzi, M. 2002, A&A, 382, 1
Papadakis, I. E., Nandra, K., & Kazanas, D. 2001, ApJ, 554, L133
Peterson, B. M., et al. 2004, ApJ, 613, 682
Remillard, R. A., & McClintock, J. E. 2006, ARA&A, 44, 49
Reynolds, C. S., et al. 2004, MNRAS, 352, 205
Romano, P., et al. 2004, ApJ, 602, 635
Santos-Lleo, M., et al. 1995, MNRAS, 270, 580
Sobolewska, M. A., Gierlinski, M., & Siemiginowska, A. 2009, MNRAS, 394, 1640
Sobolewska, M. A., Siemiginowska, A., & Åycki, P. T. 2004, ApJ, 617, 102
Sriram, K., Agrawal, V. K., Pendharkar, J. K., & Rao, A. R. 2007, ApJ, 661, 1055
Summons, D. P., Arevalo, P., McHardy, I. M., Uttley, P., & Bhaskar, A. 2007, MNRAS, 378, 649
Sunyaev, R. A., & Titarchuk, L. G. 1980, A&A, 86, 121
Uttley, P., & McHardy, I. M. 2005, MNRAS, 363, 585
Vaughan, S., Fabian, A. C., & Nandra, K. 2003, MNRAS, 339, 1237
Vaughan, S., & Nowak, M. A. 1997, ApJ, 474, L43